

Supplementary Material

Supplementary Figure 1. Fraction of intra-chromosomal interactions at different thresholds for the fifteen tissues in the study.

Supplementary Material 2. Kolmogorov-Smirnov p-values for the comparison between fraction of intra-chromosomal interactions in normal and cancer tissues at different MI thresholds.

Supplementary Figure 3. Average MI values of bins of one thousand intra-chromosomal interactions plotted against base pair distance.

Supplementary Figure 4. P-values of Wilcoxon rank sum tests comparing the distribution of MI values for bins of intra-chromosomal interactions.

Supplementary Material 5. Statistical significance of the number of intra-cytoband interactions, compared to a null model.

Supplementary Figure 6. Co-expression networks from the top 100,000 MI interactions for normal and cancer tissues.

Supplementary Figure 7. Differential expression assortativity for communities in cancer co-expression networks.

Supplementary Figure 8. Boxplots for chromosomal assortativity for GO enriched and not enriched network communities for all tissues in normal and cancer phenotypes.

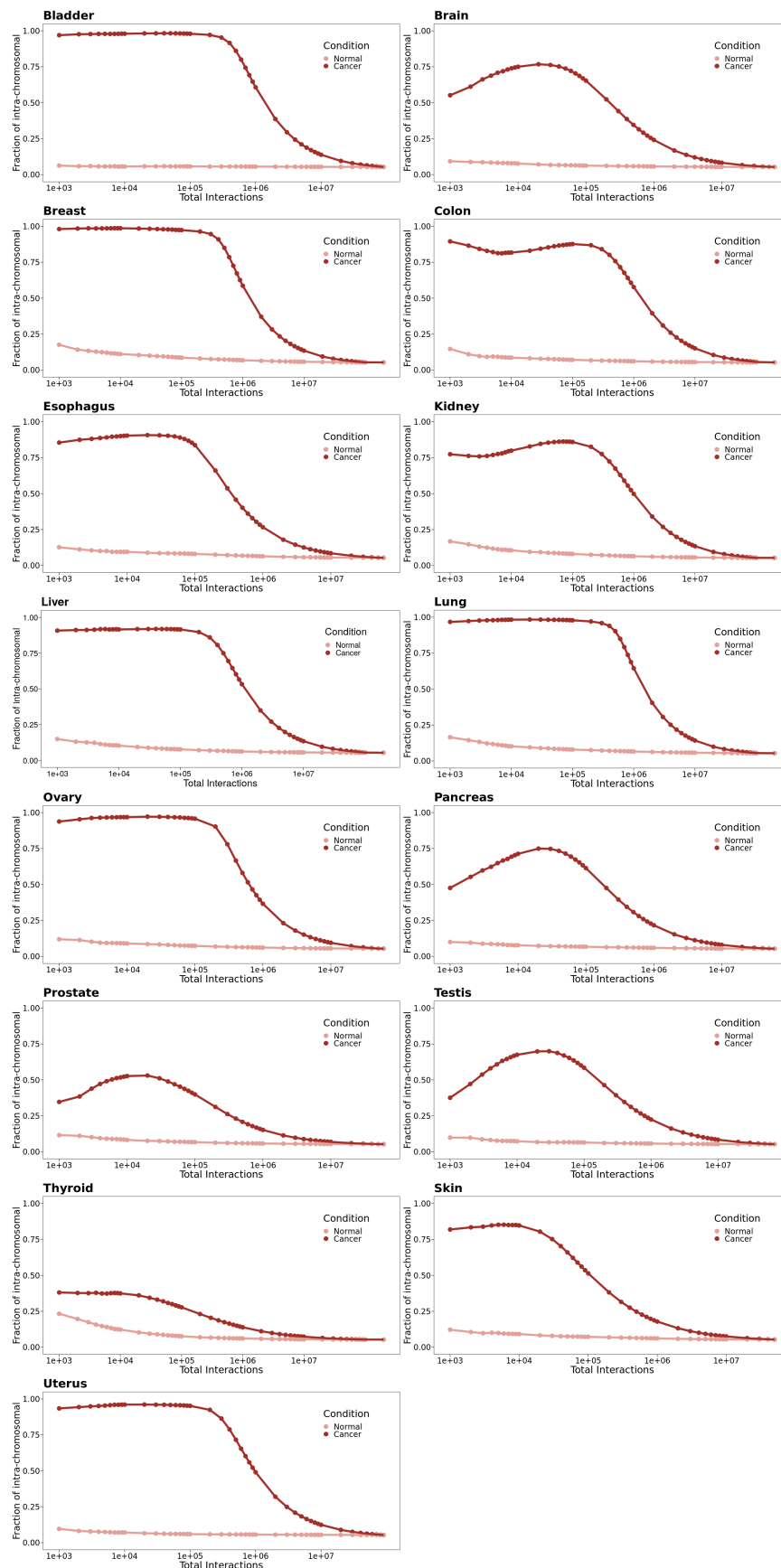
Supplementary Figure 9. HOXA-HOXB family communities in cancer with genes colored according to their differential expression.

Supplementary Figure 10. H2A, H2B family communities in cancer with genes colored according to their differential expression.

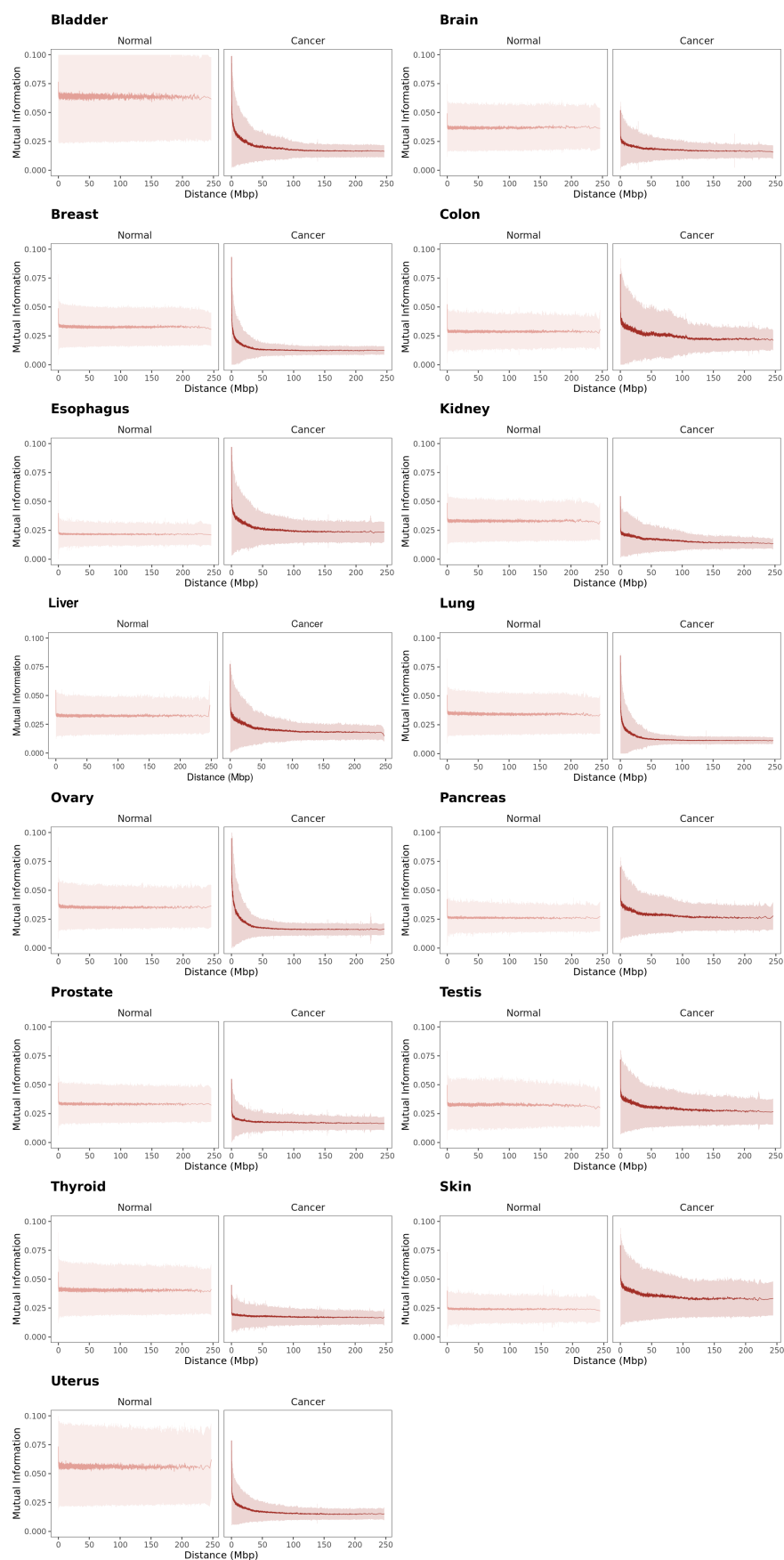
Supplementary Figure 11. PCDHG and PCDHB family communities in cancer with genes colored according to their differential expression.

Supplementary Figure 12. Unique enrichments in skin and testis normal co-expression networks with genes associated to those enrichments in cancer with their corresponding differential expression.

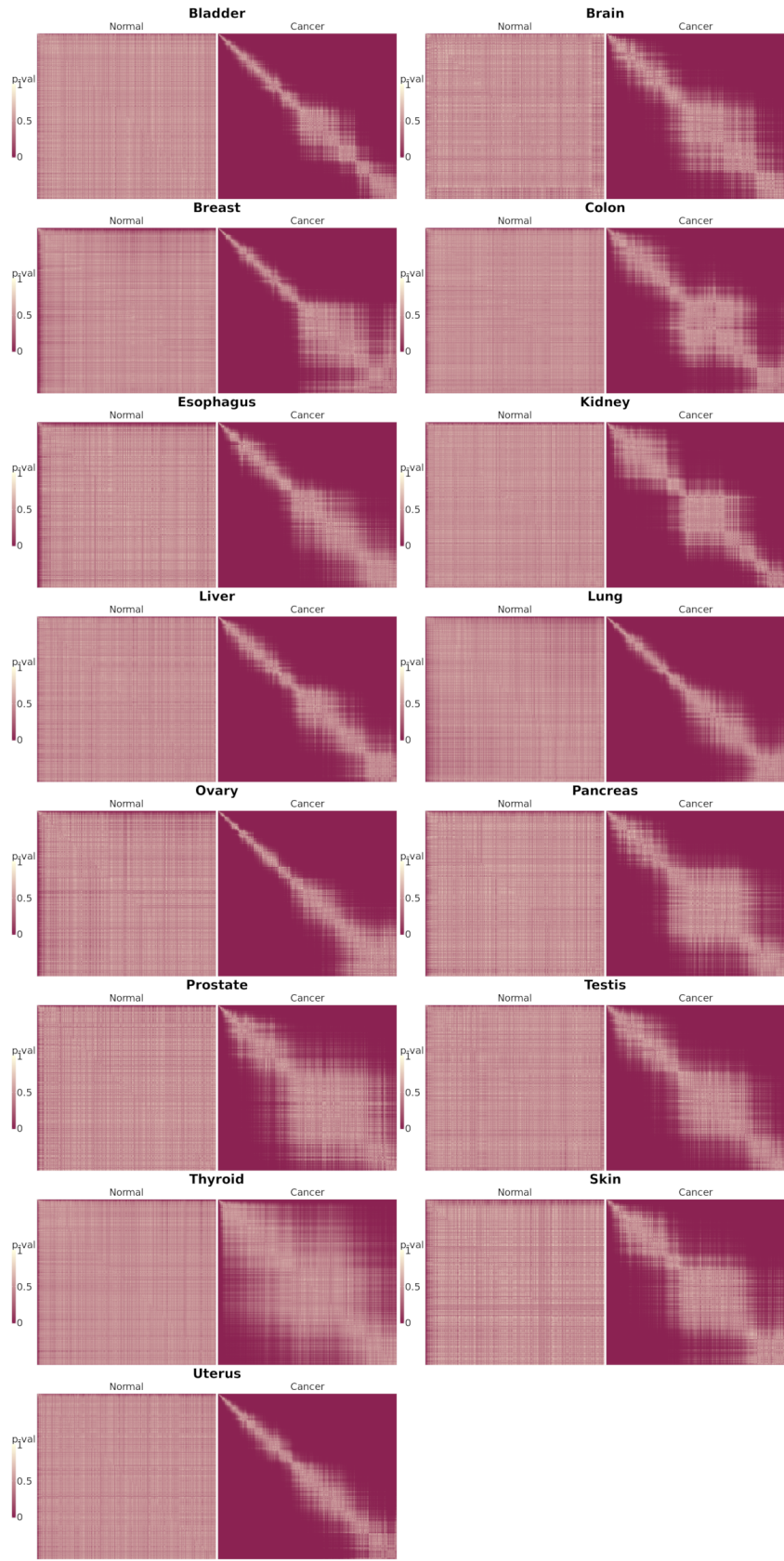
Supplementary Figure 1. Fraction of intra-chromosomal interactions at different thresholds for the fifteen tissues in the study.



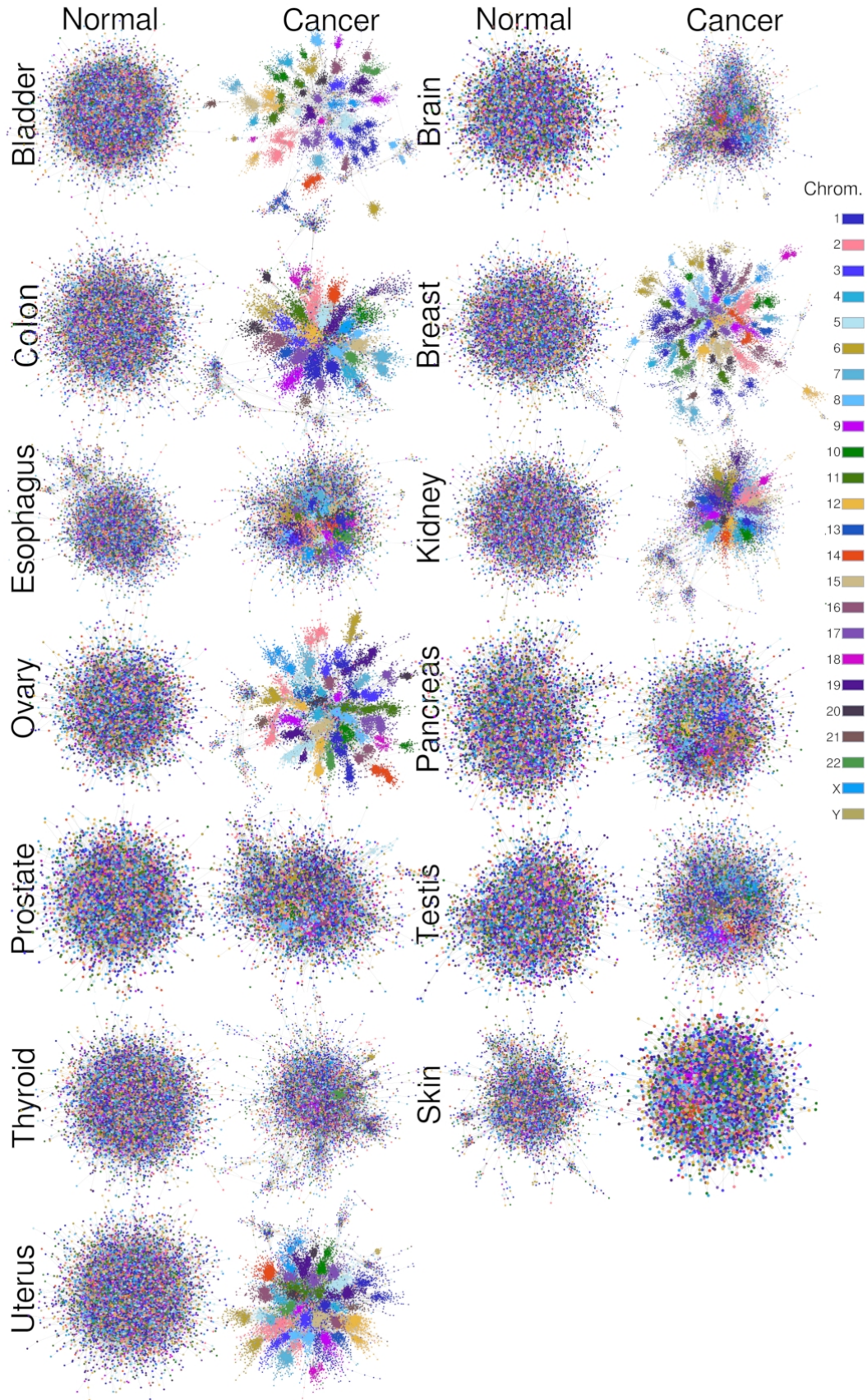
Supplementary Figure 3. Average MI values of bins of one thousand intra-chromosomal interactions plotted against base pair distance.



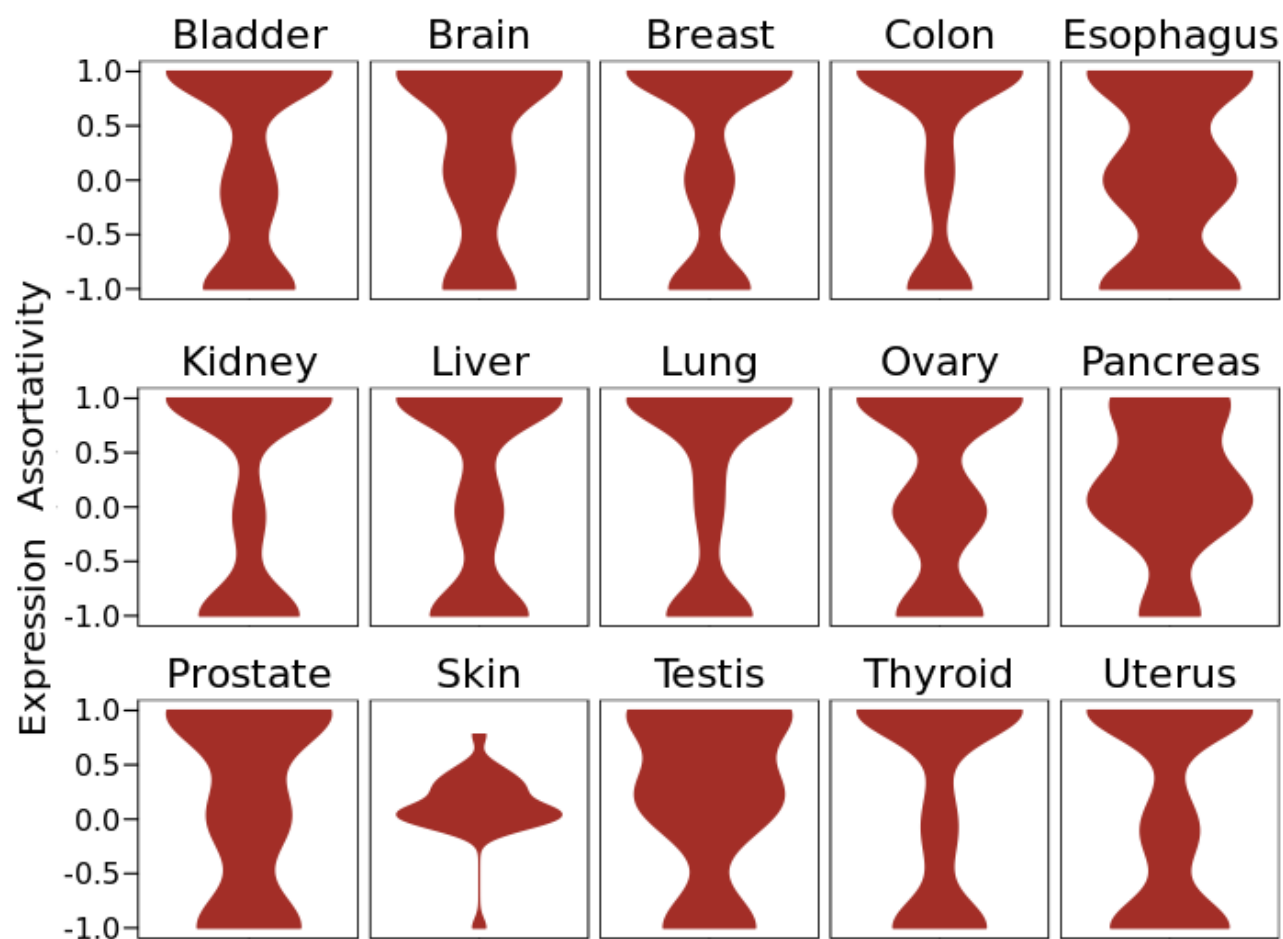
Supplementary Figure 4. P-values of Wilcoxon rank sum tests comparing the distribution of MI values for bins of intra-chromosomal interactions.



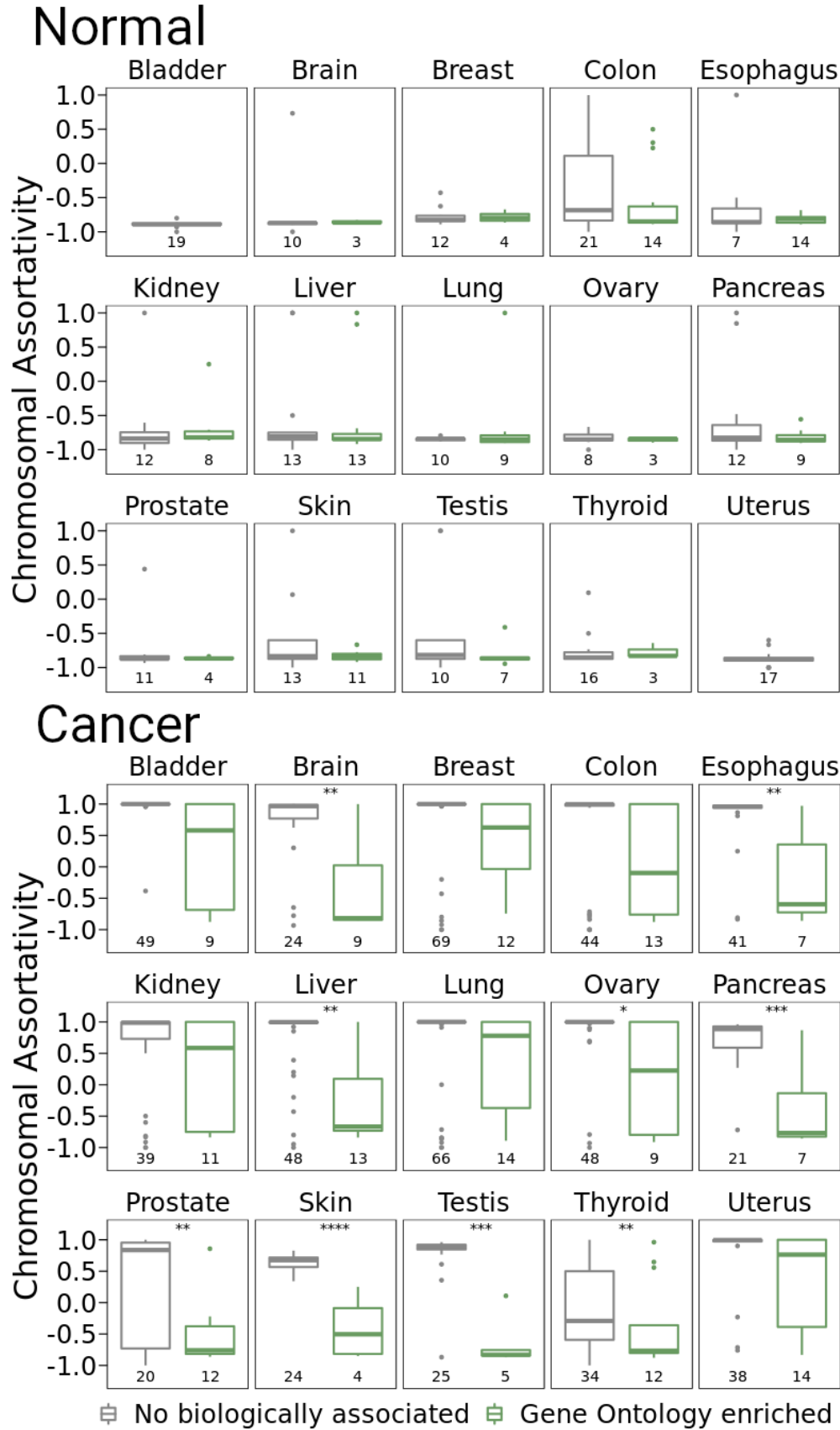
Supplementary Figure 6. Co-expression networks from the top 100,000 MI interactions for normal and cancer tissues.



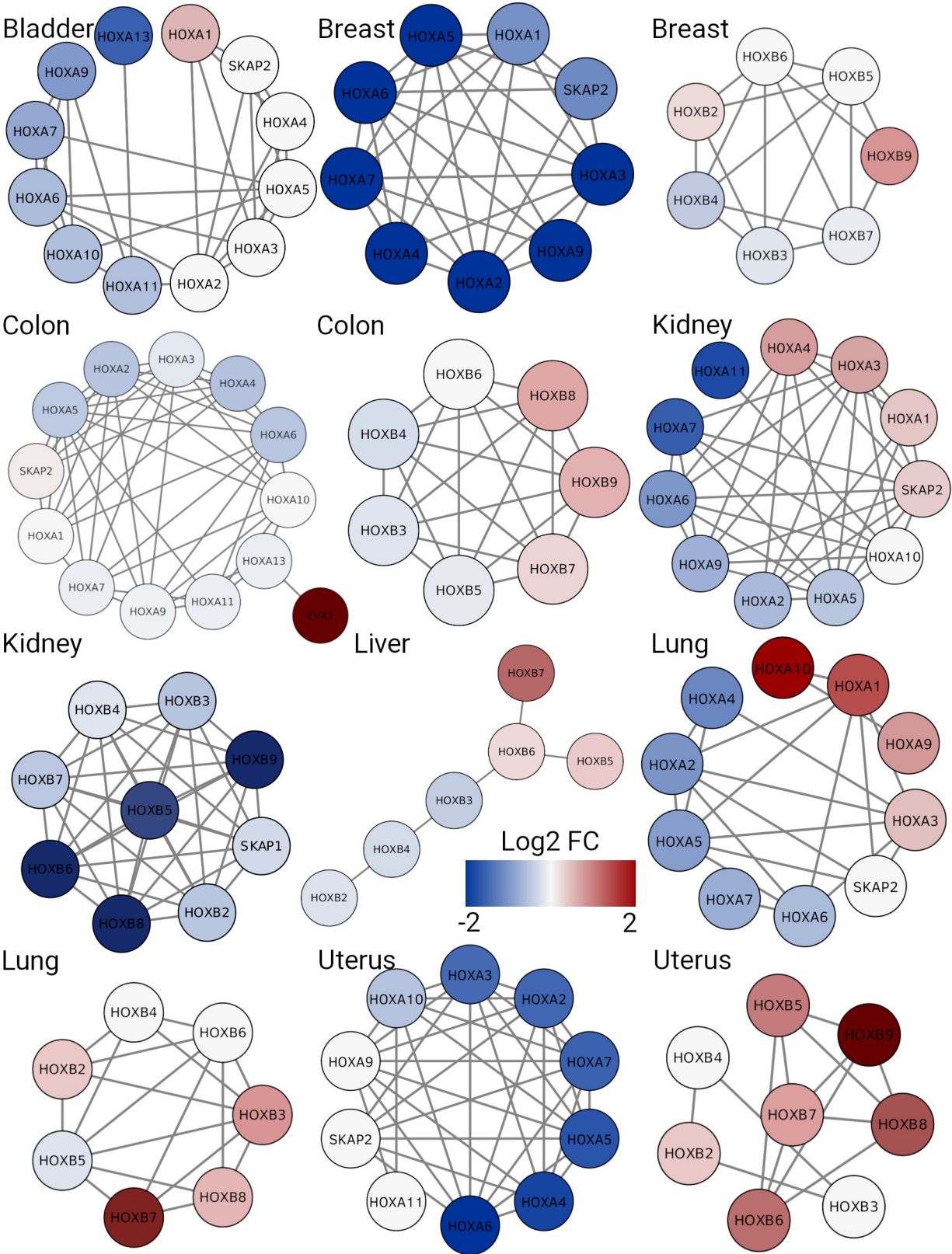
Supplementary Figure 7. Differential expression assortativity for communities in cancer co-expression networks.



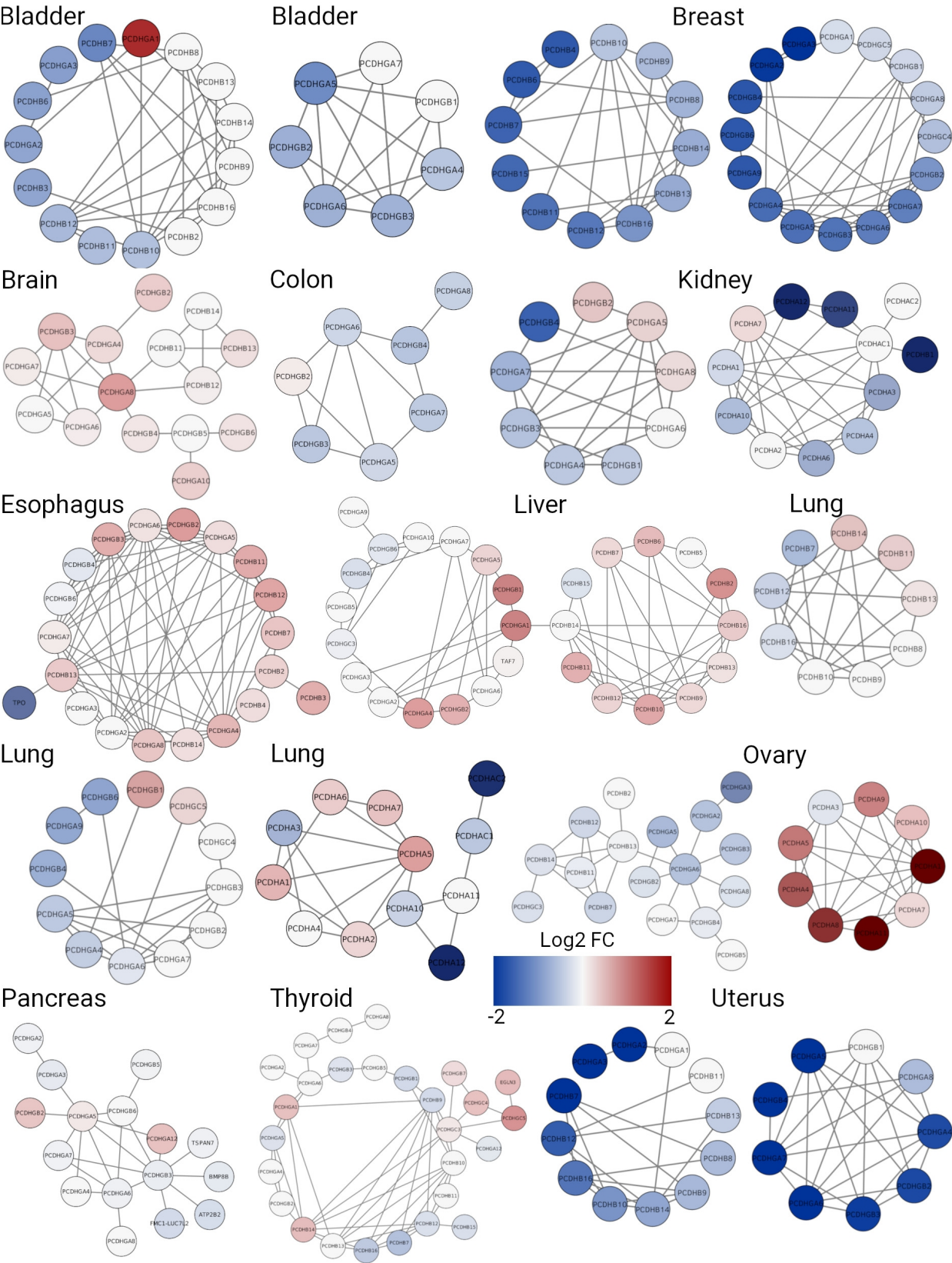
Supplementary Figure 8. Boxplots for chromosomal assortativity for GO enriched and not enriched network communities for all tissues in normal and cancer phenotypes.



Supplementary Figure 9. HOXA-HOXB family communities in cancer with genes colored according to their differential expression.



Supplementary Figure 11. PCDHG and PCDHB family communities in cancer with genes colored according to their differential expression.

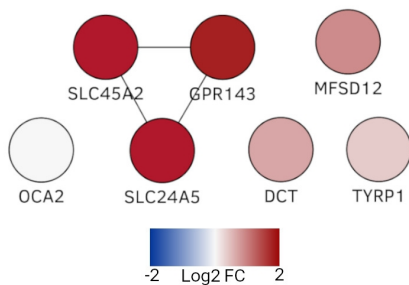


Supplementary Figure 12. Unique enrichments in skin and testis normal co-expression networks with genes associated to those enrichments in cancer with their corresponding differential expression.

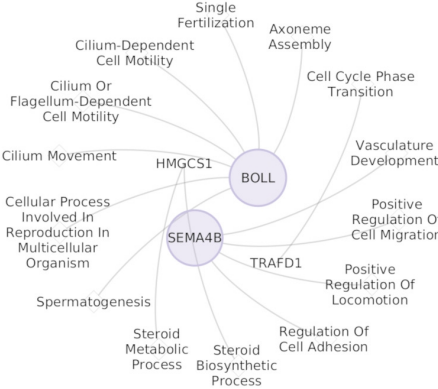
Unique GO terms in skin normal co-expression network



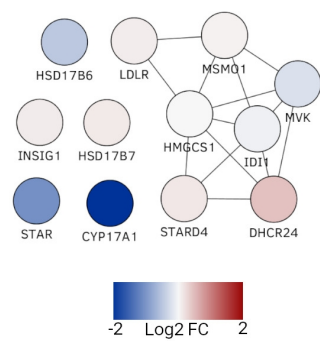
Differential expression of genes from the MLANA community enrichments in the cancer co-expression network



Unique GO terms in testis normal co-expression network



Differential expression of genes from the HMGCS1 community enrichments in the cancer co-expression network



Differential expression of genes from the BOLL community enrichments in the cancer co-expression network

